

Silane coupling agent with amine group grafted nano/micro-glass fiber as novel toughener for epoxy resin: fabrication and mechanical properties

Cuong Manh Vu, Quang-Vu Bach, Le Xuan Duong, Nguyen Viet Thai, Vu Dinh Thao, Pham Tien Duc, Dinh Duc Nguyen, Thai Hoang & Tuyen Nguyen Van

To cite this article: Cuong Manh Vu, Quang-Vu Bach, Le Xuan Duong, Nguyen Viet Thai, Vu Dinh Thao, Pham Tien Duc, Dinh Duc Nguyen, Thai Hoang & Tuyen Nguyen Van (2020): Silane coupling agent with amine group grafted nano/micro-glass fiber as novel toughener for epoxy resin: fabrication and mechanical properties, Composite Interfaces, DOI: [10.1080/09276440.2020.1729031](https://doi.org/10.1080/09276440.2020.1729031)

To link to this article: <https://doi.org/10.1080/09276440.2020.1729031>



Published online: 15 Feb 2020.



Submit your article to this journal [↗](#)



View related articles [↗](#)



View Crossmark data [↗](#)



Silane coupling agent with amine group grafted nano/micro-glass fiber as novel toughener for epoxy resin: fabrication and mechanical properties

Cuong Manh Vu^a, Quang-Vu Bach^b, Le Xuan Duong^c, Nguyen Viet Thai^c, Vu Dinh Thao^c, Pham Tien Duc^d, Dinh Duc Nguyen^e, Thai Hoang^f and Tuyen Nguyen Van^g

^aCenter for Advanced Chemistry, Institute of Research and Development, Duy Tan University, Da Nang, Vietnam; ^bSustainable Management of Natural Resources and Environment Research Group, Faculty of Environment and Labour Safety, Ton Duc Thang University, Ho Chi Minh, Vietnam; ^cChemical Department, Le Quy Don Technical University, Hanoi, Vietnam; ^dVNU University of Science, Vietnam National University, Hanoi, Vietnam; ^eDepartment of Environmental Energy & Engineering, Kyonggi University, Suwon, Republic of Korea; ^fInstitute for Tropical Technology, Vietnam Academy of Science and Technology, Hanoi, Vietnam; ^gInstitute of Chemistry, Vietnam Academy of Science and Technology, Hanoi, Vietnam

ABSTRACT

In this work, the surface of nano/micro-E-glass fibril (nGF) was modified with an amine silane coupling agent before applying as toughener for epoxy resin. The chemical structure and composition of silanized glass fibril (s-nGF) were also confirmed and compared with virgin nano/micro-glass fibrils. The curing reaction of epoxy samples with various s-nGF contents was performed at room temperature. Many characteristics of composite samples were also examined such as mechanical properties, fracture energy, thermal stability, and morphology. The experimental testing indicated that the s-nGF helps to improve the mechanical, thermal stability as well as the fracture energy of epoxy resin. The morphology observation also indicated that the s-nGF prevented the crack growth inside the epoxy matrix as the main reason of the enhancing fracture energy of epoxy resin with the presence of s-nGF.

ARTICLE HISTORY



Received 30 October 2019
Accepted 10 February 2020

KEYWORDS

Silane coupling agent; nano/micro-glass fibril; thermosetting epoxy resin; mechanical properties; fracture energy

1. Introduction

The thermosetting epoxy resins with many excellent characteristics of ease of processing, low shrinkage, high mechanical properties, and chemical resistance have been widely used in many industrial fields such as matrices for composite preparation, marine, aerospace, and automotive [1–6]. However, these resins also exhibited their brittle behavior as a result of high crosslinking density after curing, so that was limited in high performance area [7–12]. The improvement in the fracture toughness of epoxy resin has caught the attention of many researchers from around the world. The fracture energy

CONTACT Quang-Vu Bach  bachquangvu@tdtu.edu.vn  Sustainable Management of Natural Resources and Environment Research Group, Faculty of Environment and Labour Safety, Ton Duc Thang University, Ho Chi Minh, Vietnam

of epoxy resin can be enhanced by introducing the synthesized materials [13–23] or sustainable materials [24–30].

Until now, the traditional glass fiber was widely applied for both thermoplastics and thermosetting resins [31–37] due to its high mechanical properties, high chemical resistance, and compatibility with many types of organic matrices. However, there were very few works using of nano/micro-glass fiber in composite materials. The improvement of mechanical properties of epoxy resin with the presence of electro-spun nano-glass fiber and its silanized state was indicated by Chen *et al.* [38]. The nano/mirco-glass fiber with the high surface specific area was expected as the best candidate for improvement of many characteristics of epoxy resin.

In the present work, the nano/micro-glass fibril was used as toughener for epoxy resin. The amine silane coupling agent was also introduced into the surface of nano/micro-glass fiber. We also believed that the amine group in nano/micro-glass fiber can participate in the oxirane opening reaction along with diethylenetriamine (DETA) hardener.

2. Experimental section

2.1. Materials

The nano/micro-glass fiber (nGF) with trade name FM 1700 was supplied from Nippon Inorganic Colour Chem (Japan). The epoxy resin based on bisphenol A with trade name Epon 828 was purchased from Shell Chemical (USA). (3-Aminopropyl)trimethoxysilane (APS), toluene, HCl (37 wt%), diethylene tetraamine (DETA), and ethanol were also purchased from Sigma Aldrich (Vietnam). The morphology of virgin nGF was determined with the help of SEM technique as shown in Figure 1.

The diameter of nGF was varying in the range from 200 to 800 nm, while the length of nGF was from 500 to 1500 μm . The average surface area of nGF was about 56 m^2/g . The composition of E-glass fibril (nGF) is also listed in Table 1.

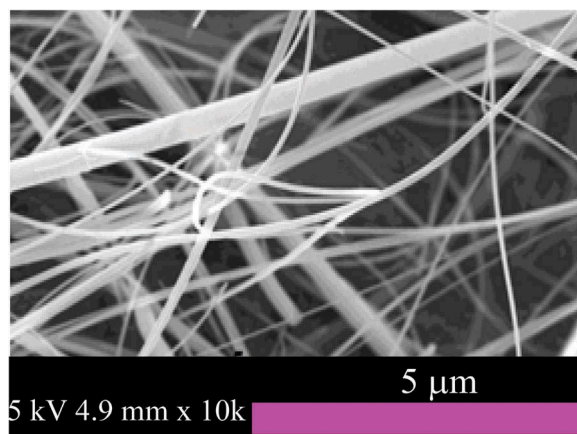


Figure 1. The morphology of nGF by SEM technique.

Table 1. The composition of E-glass fibril used in this work.

Composition	Weight (%)
SiO ₂	52.6
Al ₂ O ₃ + Fe ₂ O ₃	14.8
CaO	17.3
MgO	4.6
Na ₂ O + K ₂ O	0.9
B ₂ O ₃	9.8

2.2. s-nGF preparation

A silane coupling agent with amine group was introduced into nGF surface via our published paper [39]. About 12 g of nGF was immersed and stirred in 150 mL solution of HCl 1 M for 1 day. The pretreated nGF was washed with distilled water until neutral and then dried in a vacuum oven at 50°C for 3 h. The pretreated nGF was then also stirred in a solution of 10 mL of APS in 150 mL of toluene for 2 days. After completely silanization processing, the nGF was washed again with a mixed solvent of toluene and ethanol with ratio of 1/1 before drying in a vacuum oven for 3 h at 50°C to obtain the s-nGF.

2.3. Fabrication of s-nGF/epoxy composite

The amount of nGF and s-nGF in the epoxy resin used in this work was varying in range from 0 to 0.3 phr according to epoxy weight. The exact weight of nGF and s-nGF was first blended in the epoxy matrix with help of mechanical stirrer at 1200 rpm for 5 h. Then, these mixtures were continuously ultrasonicated for another 3 h using VC500-Vibra-Cell Ultrasonic Liquid Processors (USA). Then, these mixtures were heated in a vacuum oven at 90°C to remove the bubbles inside. The dispersion of s-nGF in epoxy resin was observed with the help of scanning electron microscopy (SEM, Jeol JSM 6360, Japan). These mixtures were then cooled to room temperature before blending with a curing agent. These mixtures were cured in a steel mold for 1 day at room temperature. After that, the epoxy samples were continuously stored at room temperature for 1 week before testing. The detail of processing is shown in Figure 2.

Also the composition detail of assigned samples is presented in Table 2.

2.4. Characterization

The chemical structure was determined with the help of Fourier transform infrared (FTIR) spectroscopy. Both nGF and s-nGF with 1 wt% according to KBr powder weight were well blended and ground with KBr before pressing to form of 12 mm disc diameter. The FTIR spectrum was obtained from the range of 400–4000 cm⁻¹ and a resolution of 1 cm⁻¹.

The chemical composition was examined using energy dispersive X-ray spectroscopy (EDS) method.

The differential scanning calorimeter (DSC-8000 PerkinElmer, USA) was used to determine the curing degree of epoxy resin. The mixtures of epoxy resin and DETA were obtained at room temperature before charging into aluminum pans, sealing, and heating from 30 to 250°C with a rate of 5°C/min. After that, the total heat of complete

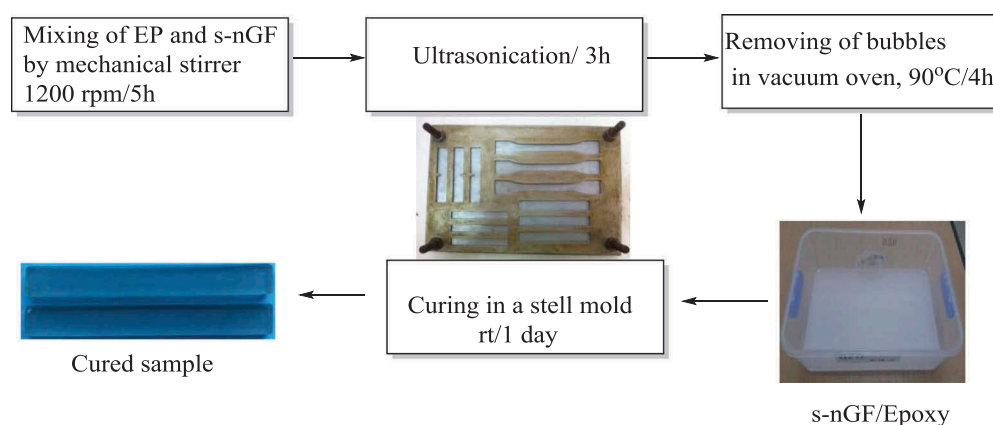


Figure 2. Multisteps for preparation of cured s-nGF/EP composite samples.

Table 2. The composition of various epoxy samples.

Sample type	EP (phr)	DETA (phr)	nGF (phr)	s-nGF (phr)
M0	100	10	–	–
M1	100	10	0.1	–
M2	100	10	0.2	–
M3	100	10	0.3	–
M4	100	10	–	0.1
M5	100	10	–	0.2
M6	100	10	–	0.3

reaction (H_T) and the residual heat of polymerization (H_R) were calculated. The curing degree can be calculate from the following equation:

$$\alpha = \frac{H_T - H_R}{H_T} \times 100\%$$

A thermogravimetric analysis (TGA) (Perkin Elmer, USA) was used to determine the thermal stability of epoxy resin. The samples were heated from 30 to 600°C under air atmosphere with a heating rate of 10°C/min and the air purge rate of 10 mL/min.

The fracture energy was determined according to ASTM D5045-99 using the following equation:

$$K_{IC} = \frac{P}{BW^{\frac{1}{2}}} f(x)$$

$$x = \frac{a}{W}$$

$$f(x) = 6x^{1/2} \frac{[1.99 - x(1-x)(2.15 - 3.93x + 2.7x^2)]}{(1+2x)(1-x)^{3/2}}$$

where P , B , W , and a are the maximum loads seen on the load–displacement diagram, the specimen thickness, the specimen width, and the initial crack length, respectively.

The tensile properties were investigated under ASTM D638-91 at room temperature with an extension rate of 2 mm/min, while the flexural properties were also determined according to ASTM D790-86. Both tensile and flexural properties were tested in a universal testing machine (Instron model 5582-100KN). All the mechanical property values were obtained by averaging five.

A dynamic mechanical analyzer (DMA8000, USA) was applied to obtain the storage modulus and tandelta of cured samples. The samples with a dimension of $50 \times 8 \times 2 \text{ mm}^3$ were heated from 30 to 200°C with a heating rate of $5^\circ\text{C}/\text{min}$ and a frequency of 1.0 Hz.

The morphologies were observed using a SEM (Jeol JSM 6360, Japan).

3. Results and discussion

The FTIR technique was used to determine the chemical structure of nGF and s-nGF as shown in Figure 3.

The results in Figure 3 indicate that both nGF and s-nGF have the same peaks at 3362, 1626, 1056, 799, 700, and 432 cm^{-1} assigned for hydroxyl group, Si–O–Si, Si–O–Al, and Si–O, respectively. The condensation reaction between silanol groups with hydroxyl groups in surface of nGF induced the reduction in the intensity of hydroxyl group at 3362, 1626, and 1056 cm^{-1} as seen in FTIR spectra of s-nGF. In addition, two peaks of CH_2 and NH_2 were realized at the peaks of 2890 and 1556 cm^{-1} . These results were also confirmed in the last published paper [40–44].

The chemical composition from EDS testing of nGF and s-nGF was also compared as shown in Figure 4.

Both nGF and s-nGF exhibited their main atoms such as Si, Al, O, and Ca. These results also were in agreement with the main components of nGF as listed in Table 1. Moreover, the existence of new peaks of C and N in the EDS spectra of s-nGF in comparison with nGF also confirmed the success of silanization processing. The atom C and N were assigned as the main component of the silane coupling agent.

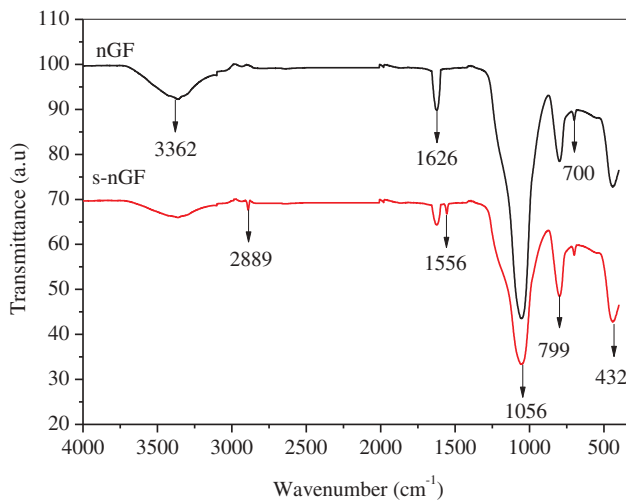


Figure 3. Comparison of the FTIR spectra of the nGF and s-nGF.

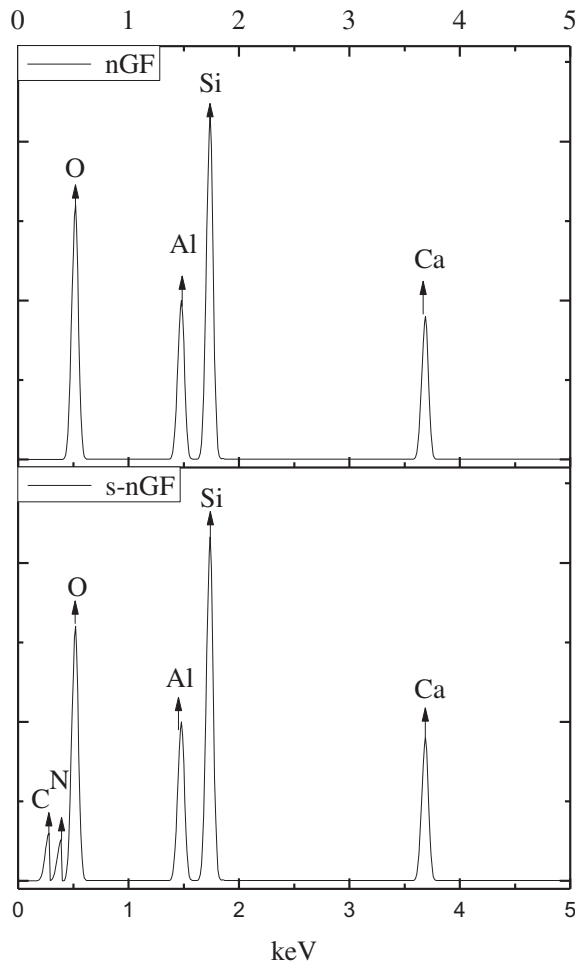


Figure 4. The chemical composition of nGF and s-nGF by EDS technique.

The dispersion of s-nGF in uncured epoxy resin was evaluated via SEM technique as shown in [Figure 5](#).

[Figure 5](#) indicates that the s-nGF was well dispersed in epoxy resin with no sign of aggregation. This result confirmed the effectiveness of silanization processing [45]. The hydrophobic of s-nGF after silanization processing with organic functional groups helps to disperse the s-nGF in epoxy resin.

The curing processing of epoxy resin has strong effect on final properties of epoxy samples. The effect of nGF and s-nGF on curing degree of epoxy resin was evaluated via DSC technique and presented in [Figure 6](#).

The results in [Figure 6](#) indicate that the curing degree increased with increasing of temperature and then reached the maximum value at around temperature from 160 to 250° C. The presence of nGF and s-nGF has different effects on the slope of these curves. The slope of the cured M5 sample with 0.2 phr s-nGF was higher than that of the slope of the M4 sample with 0.1 phr s-nGF and M0 without s-nGF. Moreover, the effect of silanization on curing degree can be evaluated via the comparison between sample M5 and sample M2 at

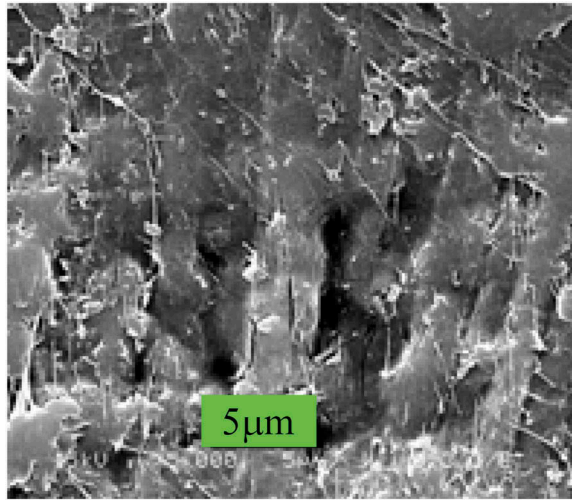


Figure 5. Observation of the dispersion of 0.3 phr s-nGF in epoxy matrix by SEM technique.

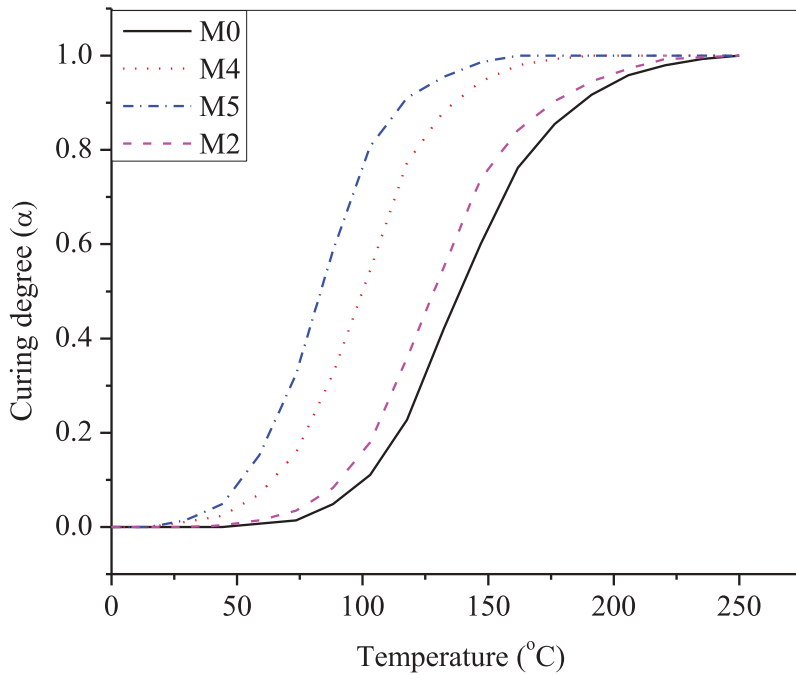


Figure 6. Plots of curing degree versus temperature with various loadings of s-nGF and nGF.

the same fibril content. The s-nGF with an amine group on its surface acted as a catalyst for ring-opening reaction of oxirane groups of epoxy resin as a result of a higher curing degree.

The effect of glass fibril content and type on fracture energy is presented in [Figure 7](#).

The fracture energy of epoxy resin increased and reached the highest value at the sample M5 with 0.2 phr of s-nGF in the epoxy matrix. The M0 sample of neat epoxy

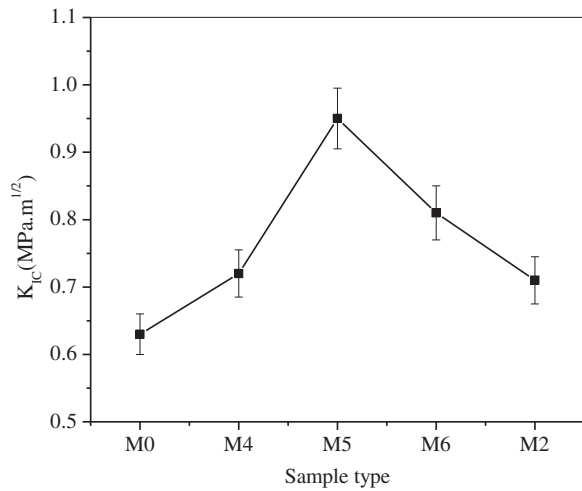


Figure 7. Effect of toughener loading on fracture energy of epoxy resin.

exhibited its lowest value of fracture energy with 0.63 ± 0.04 MPa m^{1/2}. The effect of silanization on fracture energy can be also observed via comparison between the sample M5 and M2 at the same content of glass fibril. The K_{IC} value of M5 was also higher than that of K_{IC} value of M2. The improvement of fracture energy can be expressed as the crack deflection, crack pinning process, as well as good adhesion between glass fibrils and epoxy matrix. In addition, the crack propagation can be stopped as the glass fibrils play vital role as a bridge between two surfaces of crack [46–49]. Although the fracture energy of M2 was higher than that of M0, however lower than that of M4 with 0.1 phr s-nGF. It again confirmed the effectiveness of the silanization processing in improving the fracture energy of epoxy resin. The participation of s-nGF in the epoxy network can be shown as presented in Figure 8.

The amine groups located in the surface of s-nGF can react with the oxirane groups and participate in the curing processing of epoxy matrix improve of fracture energy of epoxy resin [45]. The effectiveness of silane modification on fracture toughness of epoxy resin can also be seen in the last published papers [50–53].

The effect of glass fibril contents on flexural properties is shown in Figure 9.

In Figure 9, two peaks of flexural strength for M2 and M5 sample at the same glass fibril content of 0.2 phr are presented. However, the intensity of peak at M5 sample was also higher than that of the intensity peak of M2 as a result of the silanization effect. The same trend was also realized for the flexural modulus of the epoxy sample. The flexural strength and flexural modulus of the M5 sample increased (28.6% from 93.8 to 120.6 MPa and 30.1% from 2.06 to 2.68 GPa, respectively). While these improvement values of M2 were 10% and 2.4%, respectively. The higher values for M5 can be also expressed as the effectiveness of silanization processing and amine groups. The amine groups in s-nGF can be participated in curing reaction and make a higher number of the crosslinking bond.

The diagrams of tensile strength versus tensile strain are presented in Figure 10.

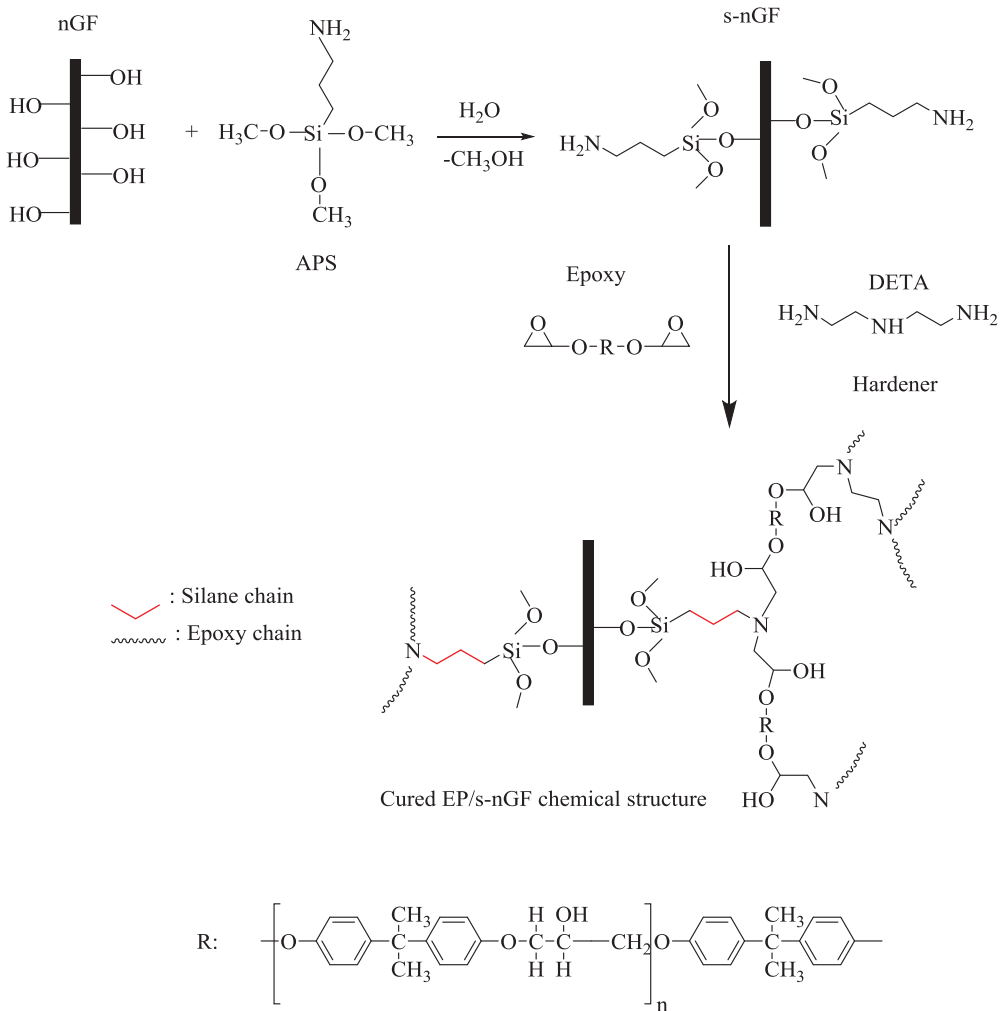


Figure 8. The way of incorporation of nGF into epoxy chain.

The slope of these curves was following the order: M6 > M5 > M4 > M2 > M0. The slope of these curves was normally in a relationship with the hardness of the composite sample. The values of tensile strength, tensile modulus, and maximum strain are also listed in Table 3.

The results in Table 3 indicate that the tensile strength of epoxy resin with the presence of s-nGF was higher than that of epoxy resin with the presence of nGF at the same content. However, both types of samples exhibited the highest value at the glass fibril content of 0.2 phr. The tensile strength, tensile modulus, and strain of the M5 sample were improved (32.67%, 23.07%, and 28.88% in comparison with the M0 sample). The decreasing trend was also observed when glass fibril content reached 0.3 phr as a result of re-agglomeration behavior. These results also were indicated in published works [54–56].

The fracture surface of epoxy samples was investigated with the help of SEM technique as shown in Figure 11.

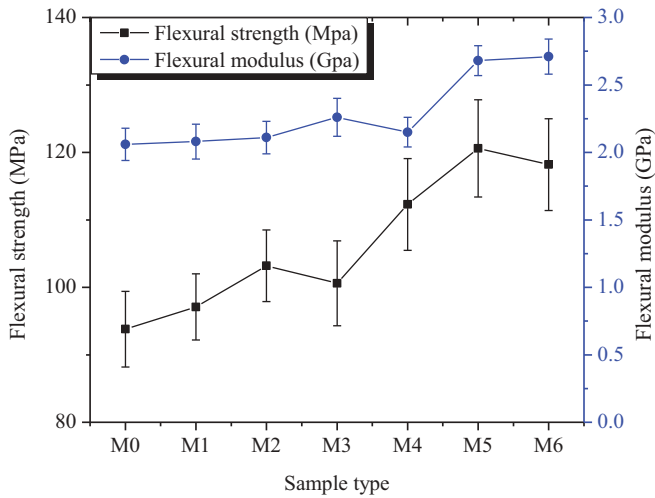


Figure 9. Effect of additive content on flexural properties of epoxy resin.

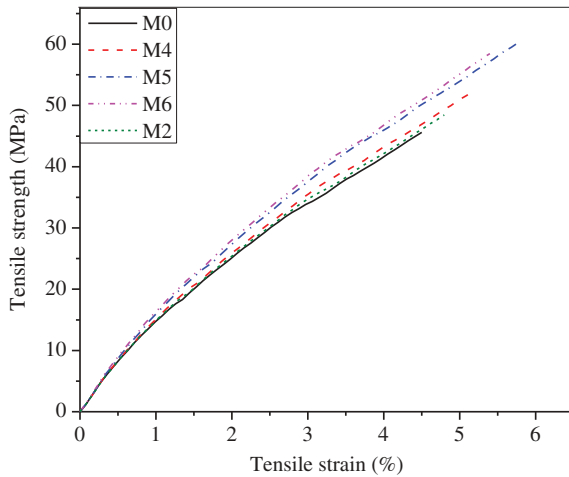


Figure 10. The relationship between tensile strength and tensile strain of various epoxy samples.

Table 3. The tensile strength, tensile modulus, and tensile strain of various epoxy samples.

Samples	Tensile strength (MPa)	Tensile modulus (GPa)	Max strain (%)
M0	45.6 ± 2.8	0.91 ± 0.06	4.5 ± 0.26
M1	48.6 ± 3.1	0.93 ± 0.05	4.6 ± 0.23
M2	51.8 ± 2.6	0.98 ± 0.06	4.8 ± 0.24
M3	50.1 ± 3.0	0.99 ± 0.05	4.7 ± 0.28
M4	52.5 ± 3.1	0.97 ± 0.06	5.2 ± 0.29
M5	60.5 ± 4.2	1.12 ± 0.08	5.8 ± 0.28

The M0 sample exhibited its smooth and glassy surface, which was characterized for brittle thermosetting resin. Both fracture surfaces of M5 and M2 samples were rougher and tougher. These results mean that more energy required for crack propagation as a

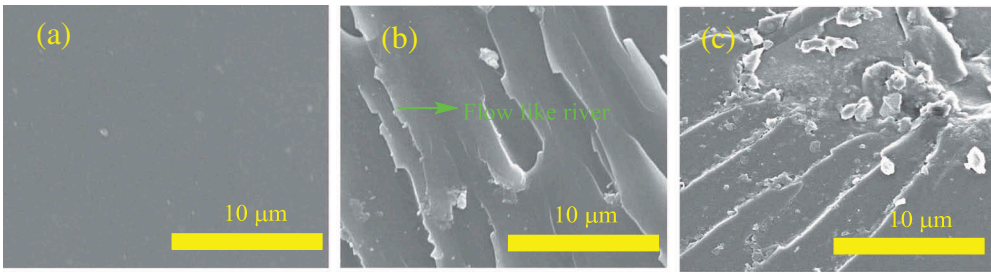


Figure 11. Evaluation fracture surface of epoxy samples by SEM technique after K_{IC} tests: (a) pristine epoxy, (b) 0.2 phr nGF/epoxy composite, and (c) 0.2 phr s-nGF/epoxy composite.

result of higher fracture energy. Moreover, the fracture surface of M5 was also rougher than that of the M2 sample. The higher interfacial interaction between s-nGF and epoxy resin in M5 sample was considered as rougher fracture surface.

The dynamic mechanical properties have strong relationship with the chemical and physical structure of epoxy composite. The influence of glass fibril content and silanization treatment on dynamic mechanical properties of epoxy resin was examined via dynamic mechanical analysis as shown in Figure 12.

Figure 12 exhibits the effect of temperature on storage modulus and tandelta of epoxy resin with different content of glass fibril. The storage modulus increased with increasing of s-nGF content. The effect of silanization on storage modulus was also realized by the comparison of the M5 and M2 samples at the same content of glass fibril. The storage modulus of the M5 sample was also higher than that of the M2 sample. This was due to the improvement of interfacial interaction between s-nGF and epoxy matrix. The strong interaction between s-nGF and epoxy matrix induced the reduction of mobility of epoxy matrix surrounding glass fibrils [51]. The tandelta of epoxy resin with various content of glass fibril is also presented in Figure 12. The same trend as storage modulus was also realized. The intensity peak of tandelta was increased with increase of s-nGF content. The temperature at the peak of tandelta was considered as a glass transition temperature (T_g) of epoxy resin. The T_g value of epoxy resin for M0, M4, M5, and M6 were 97.7, 99.6, 100.3, and 103.9°C, respectively. The improvement of T_g was due to the reduction of mobility of epoxy chain which was induced by the increase of interfacial interaction between epoxy matrix and s-nGF.

The effect of glass fibril and silanization processing on thermal stability of epoxy resin was determined with help of TGA analyzer as shown in Figure 13.

The results in Figure 13 point out that the main degradation of epoxy network expressed at around 350–500°C [46]. The decomposition temperature (T_d , at 5.0 wt% weight loss) of virgin epoxy resin and epoxy resin with the presence of 0.2 phr nGF and 0.2 phr s-nGF were 270, 290, and 294°C, respectively. The higher T_d value of epoxy resin with the presence of s-nGF in comparison with nGF confirmed again the effectiveness of silanization. The good dispersion and covalent bonds between glass fibril and epoxy matrix were considered as the main reason for enhancing the thermal properties of M5 sample [46]. In addition, the formation of SiO_2 after the decomposition of the silane coupling agent was the cause by higher char residue of M5 sample in comparison with the M2 sample.

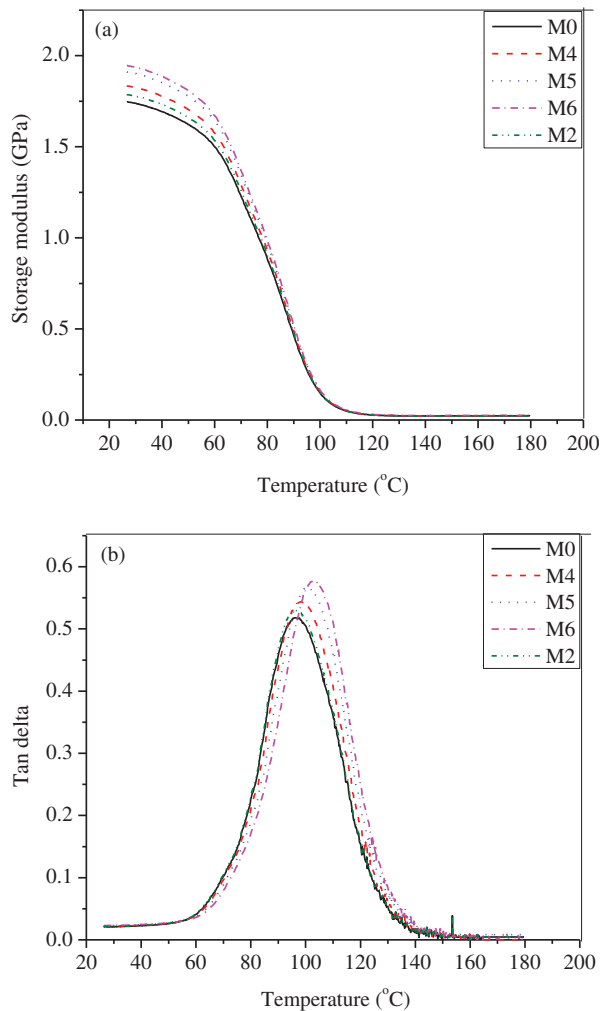


Figure 12. Storage modulus and tandelta of various epoxy samples.

4. Conclusion

In the present work, the silanized nano/micro-glass fibril (s-nGF) was synthesized before using as reinforcement for epoxy resin. The experimental fracture energy and mechanical properties of epoxy resin were improved with three kinds of content of s-nGF from 0.1 to 0.3 phr. The presence of s-nGF also induced the improvement of the thermal stability of epoxy resin. The SEM technique was applied to evaluate the fracture surface and confirm the enhancement of fracture energy. The rougher surface with multi-growth as flow rivers of epoxy resin with the presence of s-nGF was considered as the main reason of improvement of fracture energy. In addition, the s-nGF also participated in the curing reaction of epoxy chains via an opening reaction between amine groups and oxirane groups. The glass transition temperature and storage modulus of epoxy resin were also improved with presence of s-nGF.

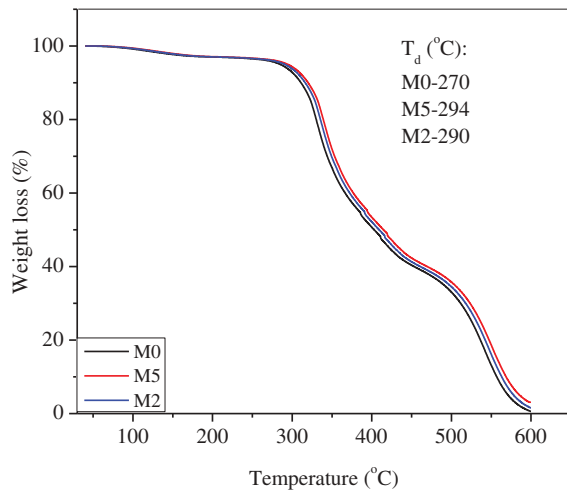


Figure 13. Thermal stability of various epoxy samples.

Disclosure statement

No potential conflict of interest was reported by the authors.

Funding

This research was funded by the Vietnam National Foundation for Science and Technology Development (NAFOSTED) : [Grant Number 104.02-2017.15].

References

- [1] Vu CM, Choi HJ. Fracture toughness and surface morphology of micro/nano sized fibrils-modified epoxy resin. *Polym Sci Ser A*. 2016;58:464–470.
- [2] Vu CM, Nguyen LT, Nguyen TV, et al. Effect of additive-added epoxy on mechanical and dielectric characteristics of glass fiber reinforced epoxy composites. *Polym Kor*. 2014;38:726–734.
- [3] Vu CM, Nguyen TV, Nguyen LT, et al. Fabrication of adduct filled glass fiber/epoxy resin laminate composites and their physical characteristics. *Polym Bull*. 2016;73:1373–1391.
- [4] Pham TD, Vu CM, Choi HJ. Enhanced fracture toughness and mechanical properties of epoxy resin with rice husk-based nano-silica. *Polym Sci Ser A*. 2017;59:437–444.
- [5] Vu CM, Nguyen DD, Pham TD, et al. Environmentally benign green composites based on epoxy resin/bacterial cellulose reinforced glass fiber: fabrication and mechanical characteristics. *Polym Test*. 2017;61:150–161.
- [6] Vu CM, Choi HJ, Pham TD. Effect of micro/nano white bamboo fibrils on physical characteristics of epoxy resin reinforced composites. *Cellulose*. 2017;24:5475–5486.
- [7] Vu CM, Nguyen DD, Choi HJ, et al. Micro-fibril cellulose as a filler for glass fiber reinforced unsaturated polyester composites: fabrication and mechanical characteristics. *Macromol Res*. 2018;26:54–60.
- [8] Hoang SL, Vu CM, Pham LT, et al. Preparation and physical characteristics of epoxy resin/bacterial cellulose biocomposites. *Polym Bull*. 2018;75:2607–2625.

- [9] Nguyen LT, Vu CM, Phuc BT, et al. Simultaneous effects of silanized coal fly ash and nano/micro glass fiber on fracture toughness and mechanical properties of carbon fiber-reinforced vinyl ester resin composites. *Polym Eng Sci.* **2019**;59:584–591.
- [10] Bach QV, Vu CM, Vu HT, et al. Significant enhancement of fracture toughness and mechanical properties of epoxy resin using CTBN-grafted epoxidized linseed oil. *J Appl Polym Sci.* **2020**;137:48276.
- [11] Vu CM, Nguyen VH, Bach QV. Phosphorous-jointed epoxidized soybean oil and rice husk-based silica as the novel additives for improvement mechanical and flame retardant of epoxy resin. *J Fire Sci.* **2020**;073490411990099. DOI:10.1177/0734904119900990
- [12] Bach QV, Vu CM, Vu HT, et al. Enhancing mode I and II interlaminar fracture toughness of carbon fiber-filled epoxy-based composites using both rice husk silica and silk fibroin electrospun nanofibers. *High Perform Polym.* **2019**;31:1195–1203.
- [13] Wang L, Tan Y, Wang H, et al. Investigation on fracture behavior and mechanisms of DGEBF toughened by CTBN. *Chem Phys Lett.* **2018**;699:14–21.
- [14] Jiang M, Liu Y, Cheng C, et al. Enhanced mechanical and thermal properties of mono-component high performance epoxy resin by blending with hydroxyl terminated polyether-sulfone. *Polym Test.* **2018**;69:302–309.
- [15] Cheng C, Chen Z, Huang Z, et al. Simultaneously improving mode I and mode II fracture toughness of the carbon fiber/epoxy composite laminates via interleaved with uniformly aligned PES fiber webs. *Compos A: Appl Sci Manuf.* **2020**;129:105696.
- [16] Prasad T, Halder S, Dhar SS. Imidazole-supported silica one-pot processed nanoparticles to enhance toughness of epoxy based nanocomposites. *Mater Chem Phys.* **2019**;231:75–86.
- [17] Picu CR, Krawczyk KK, Wang Z, et al. Toughening in nanosilica-reinforced epoxy with tunable filler-matrix interface properties. *Compos Sci Tech.* **2019**;183:107799.
- [18] Peng J, Huang C, Cao C, et al. Inverse nacre-like epoxy-graphene layered nanocomposites with integration of high toughness and self-monitoring. *Matter.* **2020**;2:220–232.
- [19] Elmarakbi A, Karagiannidis P, Ciappa A, et al. 3-phase hierarchical graphene-based epoxy nanocomposite laminates for automotive applications. *J Mater Sci Tech.* **2019**;35:2169–2177.
- [20] Yan M, Jiao W, Ding G, et al. High strength and toughness epoxy nanocomposites reinforced with graphene oxide-nanocellulose micro/nanoscale structures. *Appl Surf Sci.* **2019**;497:143802.
- [21] Li J, Zhu W, Zhang S, et al. Amine-terminated hyperbranched polyamide covalent functionalized graphene oxide-reinforced epoxy nanocomposites with enhanced toughness and mechanical properties. *Polym Test.* **2019**;76:232–244.
- [22] Wang TT, Huang P, Li YQ, et al. Epoxy nanocomposites significantly toughened by both poly(sulfone) and graphene oxide. *Compos Commun.* **2019**;14:55–60.
- [23] Klingler A, Bajpai A, Wetzel B. The effect of block copolymer and core-shell rubber hybrid toughening on morphology and fracture of epoxy-based fibre reinforced composites. *Eng Fract Mech.* **2018**;203:81–101.
- [24] Wang J, Pozegic TR, Xu Z, et al. Cellulose nanocrystal-polyetherimide hybrid nanofibrous interleaves for enhanced interlaminar fracture toughness of carbon fibre/epoxy composites. *Compos Sci Tech.* **2019**;182:107744.
- [25] Yeo JS, Kim OY, Hwang SH. The effect of chemical surface treatment on the fracture toughness of microfibrillated cellulose reinforced epoxy composites. *J Indus Eng Chem.* **2017**;45:301–306.
- [26] Kalali EN, Hu Y, Wang X, et al. Highly-aligned cellulose fibers reinforced epoxy composites derived from bulk natural bamboo. *Indust Crops Prod.* **2019**;129:434–439.
- [27] Saba N, Safwan A, Sanyang ML, et al. Thermal and dynamic mechanical properties of cellulose nanofibers reinforced epoxy composites. *Inter J Bioll Macromol.* **2017**;102:822–828.
- [28] Kuo PY, Barros LA, Yan N, et al. Nanocellulose composites with enhanced interfacial compatibility and mechanical properties using a hybrid-toughened epoxy matrix. *Carbo Polym.* **2017**;177:249–257.

- [29] Baruah P, Karak N. Bio-based tough hyperbranched epoxy/graphene oxide nanocomposite with enhanced biodegradability attribute. *Polym Degrad Stab.* **2016**;129:26–33.
- [30] Ferdosian F, Zhang Y, Yuan Z, et al. Curing kinetics and mechanical properties of bio-based epoxy composites comprising lignin-based epoxy resins. *Eur Polym J.* **2016**;82:153–165.
- [31] Ahmedizat SR, Zubaidi AA, Tabbakh AAA, et al. Comparative study of erosion wear of glass fiber/epoxy composite reinforced with Al₂O₃ nano and micro particles. *Mater Today.* **2020**;20:420–427.
- [32] Bagci M, Demirci M, Sukur EF, et al. The effect of nanoclay particles on the incubation period in solid particle erosion of glass fibre/epoxy nanocomposites. *Wear.* **2020**;444–445:203159.
- [33] Hagenbeek M, Sinke J. Effect of long-term thermal cycling and moisture on heated Fibre Metal Laminates and glass-fibre epoxy composites. *Compos Struct.* **2019**;210:500–508.
- [34] Rungruangsuparat S, Patcharaphun S, Sombatsompop N. Materials modification and die design for minimizing internal melt distortions of glass fiber/PP co-extrudates. *Polym Test.* **2017**;57:184–191.
- [35] Sorrentino L, Simeoli G, Iannace S, et al. Mechanical performance optimization through interface strength gradation in PP/glass fibre reinforced composites. *Compos B: Eng.* **2015**;76:201–208.
- [36] Fu SY, Lauke B, Li RKY, et al. Effects of PA6,6/PP ratio on the mechanical properties of short glass fiber reinforced and rubber-toughened polyamide 6,6/polypropylene blends. *Compos B: Eng.* **2006**;37:182–190.
- [37] Güllü A, Özdemir A, Özdemir E. Experimental investigation of the effect of glass fibres on the mechanical properties of polypropylene (PP) and polyamide 6 (PA6) plastics. *Mater Desig.* **2006**;27:316–323.
- [38] Chen Q, Zhang L, Yoon MK, et al. Preparation and evaluation of nano-epoxy composite resins containing electrospun glass nanofibers. *J Appl Polym Sci.* **2012**;124:444–451.
- [39] Park DE, Choi HJ, Vu CM. Stimuli-responsive polyaniline coated silica microspheres and their electrorheology. *Smart Mater Struct.* **2016**;25:055020.
- [40] Gebald C, Wurzbacher JA, Tingaut P, et al. Stability of amine-functionalized cellulose during temperature vacuum-swing cycling for CO₂ capture from air. *Environ Sci Technol.* **2013**;47:10063–10070.
- [41] Ishida H, Koenig JL. Fourier transform infrared spectroscopic study of the structure of silane coupling agent on E-glass fiber. *J Colloid Interf Sci.* **1978**;64:565–576.
- [42] Ishida H, Koenig JL. An investigation of the coupling agent/matrix interface of fiberglass reinforced plastics by fourier transform infrared spectroscopy. *J Polym Sci Phys.* **1979**;17:615–626.
- [43] Ishida H, Koenig JL. Effect of hydrolysis and drying on the siloxane of a silane coupling agent deposited on E-glass fibers. *J Polym Sci Phys.* **1980**;18:233–237.
- [44] Ishida H, Koenig JL. The structure of γ -aminopropyltriethoxysilane on glass surfaces. *J Colloid Interface Sci.* **1980**;74:396–404.
- [45] Gholami S, López J, Rezvani A, et al. Fabrication of thin-film nanocomposite nanofiltration membranes incorporated with aromatic amine-functionalized multiwalled carbon nanotubes. Rejection performance of inorganic pollutants from groundwater with improved acid and chlorine resistance. *Chem Eng J.* **2020**;384:123348.
- [46] Wang Q, Shi W, Zhu B, et al. An effective and green H₂O₂/H₂O/O₃ oxidation method for carbon nanotube to reinforce epoxy resin. *J Mater Sci Tech.* **2020**;40:24–30.
- [47] Wu W, Xu Y, Wu H, et al. Synthesis of modified graphene oxide and its improvement on flame retardancy of epoxy resin. *J Appl Polym Sci.* **2020**;137:47710.
- [48] Han S, Meng Q, Araby S, et al. Mechanical and electrical properties of graphene and carbon nanotube reinforced epoxy adhesives: experimental and numerical analysis. *Compos A: Appl Sci Manuf.* **2019**;120:116–126.
- [49] Ferreira FV, Brito FS, Franceschi W, et al. Functionalized graphene oxide as reinforcement in epoxy based nanocomposites. *Surf Interf.* **2018**;10:100–109.

- [50] Ramezanzadeh M, Ramezanzadeh B, Sari MG, et al. Corrosion resistance of epoxy coating on mild steel through polyamidoamine dendrimer-covalently functionalized graphene oxide nanosheets. *J Indus Eng Chem.* [2020](#);82:290–302.
- [51] Damian CM, Necolau MI, Neblea I, et al. Synergistic effect of graphene oxide functionalized with SiO₂ nanostructures in the epoxy nanocomposites. *Appl Surf Sci.* [2020](#);507:145046.
- [52] Liu M, Zhang C, Tjiu WW, et al. One-step hybridization of graphene nanoribbons with carbon nanotubes and its strong-yet-ductile thermoplastic polyurethane composites. *Polym.* [2013](#);54:3124–3130.
- [53] Wu Q, Gong LX, Li Y, et al. Efficient flame detection and early warning sensors on combustible materials using hierarchical graphene oxide/silicone coatings. *ACS Nano.* [2018](#);12:416–424.
- [54] Kuilla T, Bhadra S, Yao D, et al. Recent advances in graphene based polymer composites. *Prog Polym Sci.* [2010](#);35:1350–1375.
- [55] Boland CS, Barwich S, Khan U, et al. High stiffness nanocomposite fibres from polyvinylalcohol filled with graphene and boron nitride. *Carbon.* [2016](#);99:280–288.
- [56] Domun N, Hadavini H, Zhang T, et al. Improving the fracture toughness properties of epoxy using graphene nanoplatelets at low filler content. *Nanocompos.* [2017](#);3:85–96.